Effects of Tip Clearance Size on Active Control of Turbine Tip Clearance Flow Using Ring-type DBD Plasma Actuators

Takayuki Matsunuma[1]*, Takehiko Segawa[1]

ISROMAC 2017

International Symposium on Transport Phenomena and Dynamics of Rotating Machinery

Hawaii, Maui

December 16-21 2017

Abstract

Ring-type dielectric barrier discharge (DBD) plasma actuators have been developed to facilitate active control of the tip leakage flow of a turbine rotor. In order to construct a two-dimensional model of the tip leakage flow, a flat plate was inserted with a certain clearance between rectangular test section of a wind tunnel and velocity distributions near the plate tip regions were analyzed by particle image velocimetry (PIV). In this study, effects of the tip clearance size of the flat plate were examined at different tip clearance sizes from 0.6 mm to 2.4 mm in a wind tunnel at low tip leakage velocity conditions of 1 m/s - 2 m/s. The input voltage and frequency were varied in the ranges between 10 kV and 17 kV, 2 kHz and 12 kHz, respectively. The forcibly-induced tip leakage flow was easily dissipated at smaller tip clearance size (0.6 mm and 1.0 mm) by applying relatively smaller input voltage. The larger tip clearance size requires the higher applied voltage and frequency in order to reduce the tip leakage flow. At larger tip clearance of 1.8 mm, the mass flow rate of the tip leakage flow is increased and the flow diffusion is observed at the low frequency operation, 2 kHz. At the largest tip clearance of 2.4 mm, the peak velocity of the tip leakage flow is 38% reduced by the effect of the plasma actuator of the input voltage of 17 kV and frequency of 10 kHz.

Keywords

Plasma actuator, DBD, Active flow control, Turbine, Tip clearance, Tip leakage flow

[1]*National Institute of Advanced Industrial Science and Technology (AIST), Tsukuba, Japan*

***Corresponding author**: t-matsunuma@aist.go.jp

INTRODUCTION

Tip clearance between the blade tips and the casing in turbomachinery induces leakage flow, which arises due to the pressure difference between the pressure surface and the suction surface of the blade. The leakage flow emerging from the clearance interacts with the passage flow and rolls up into a vortex known as the “tip leakage vortex.” Although the size of the clearance is typically about one percent of the blade height, the leakage flow through this small clearance has a significant effect on the aerodynamics of the turbine. For example, the tip clearance loss of a turbine blade can account for as much as from 20 to 40% of the total losses [1]. The loss of performance due to tip clearance flow has therefore been intensively studied for many years. Booth [1] and more recently Sjolander [2] presented comprehensive reviews of the various effects of tip clearance flow. Bindon [3], Dishart and Moore [4], Yaras and Sjolander [5], and Heyes and Hodson [6] made detailed measurements of the tip clearance flow. In addition, Heyes et al. [7] and Morphis and Bindon [8] investigated the effect of tip geometry. Concurrently, numerous studies focusing on loss prediction methods have been conducted, over a long period [9]-[14].

The basic structure of dielectric barrier discharge (DBD) for flow control was described by Roth et al. [15] in 1998, and the application of DBD plasma actuators has been developed over the last decade, from fundamental studies to a wide range of applications [16]; among these, major targets are separation control [17]-[21] and drag reduction [22]. With regard to tip clearance flow control, Van Ness II et al. [23]-[25] investigated the effect of active control using blade-tip-mounted plasma actuators.

RING-TYPE PLASMA ACTUATOR

Figures 1 shows the new ring-type plasma actuator for tip

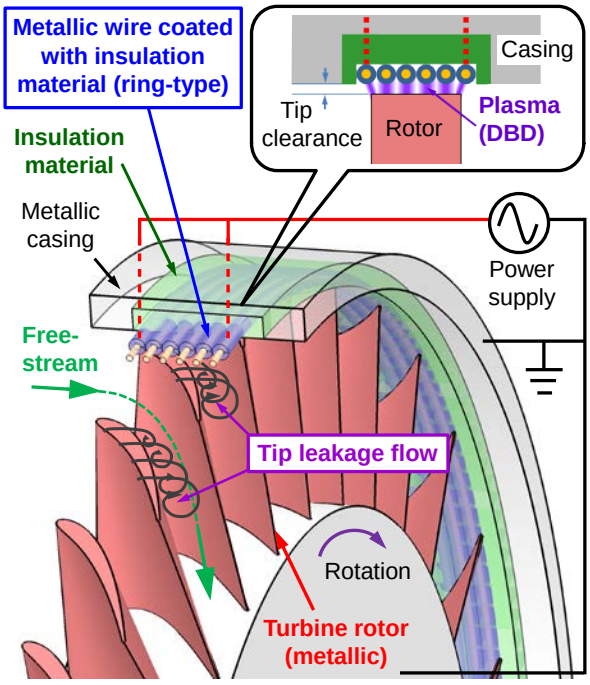

Figure 1. Ring-type plasma actuator

clearance flow reduction in an axial-flow turbine rotor. Metallic wires coated with insulation material, to which high voltages are applied, are mounted in a ring-shaped insulator embedded in the casing (tip endwall). All of the conductive materials, such as the turbine blades, drive shaft, and casing wall, are connected to the ground for safety. When high voltages at high frequencies are applied to the metallic wires, the tip of the turbine rotor takes on the role of a ground electrode, and glow discharge plasma is formed between the metal wire in the casing wall and the tip of the turbine blades. The induced flow by the glow discharge plasma blocks the tip leakage flow when such a ring-type plasma actuator is used for tip leakage flow control in a turbine rotor [26].

The ring-type plasma actuator can also be widely applied to the active control of various rotating machines, such as axial compressors, centrifugal compressors, radial turbines, and labyrinth seals, for tip leakage flow reduction and stall margin improvement.

EXPERIMENTAL METHODS

Figure 2 shows the 500 mm x 200 mm x 200 mm test section of a low-speed, open-circuit, blower-type system. A metallic flat plate (10 mm thickness) was installed in the test section of the wind tunnel with various tip clearance sizes (0.6 mm - 2.4 mm) at the bottom end. As shown in Fig. 3, a string-type plasma actuator array (140 mm x 140 mm) was attached to the acrylic bottom endwall as a two-dimensional model of a ring-type plasma actuator. The metallic wires coated with silicone rubber of the plasma actuator run perpendicular to the metal plate. The plasma actuator array was excited with quasi-rectangular waveform from a power supply (HAPS-10B40, Matsusada Precision Inc.). The metallic flat plate was connected to ground, V_g = 0 V. The input voltage and frequency to the string-type plasma actuator was changed in this study. Generally, both an increase in voltage and an increase in frequency result in stronger plasma generation.

For the flat plate experiments in a wind tunnel, the tip leakage flow was forcibly induced at the tip clearance of the flat plate. In order to avoid unstable operation of the wind tunnel due to resistance of the air flow by the flat plate, a slit for bypass flow was opened in the upstream top wall of the test section, as shown in Fig. 2.

Particle image velocimetry (PIV) was used to obtain two-dimensional velocity field near the plate tip clearance regions (purple frame in Fig. 2), using a 25 mJ/pulse, double-pulse Nd-YAG laser (MiniLase II, 20 Hz, New Wave Research Co., Ltd.). The thickness of the laser sheet was less than 1 mm. Atomized dioctyl sebacate (DOS) oil with a mean particle diameter of 1 μm was injected upstream of the test section, via a pressurized oil chamber. Image pairs were taken by a camera (PIV CAM 13-8, TSI, Inc.) with 1,280 x 1,024 pixel resolution and a frame rate of 3.75 Hz. TSI software calculated the velocity vectors from the peak correlation of groups of particles between frames, using conventional cross-correlation algorithms on a 32 x 32 pixel grid. In order to calculate the time-averaged velocity distributions, 300 instantaneous velocity distributions were measured.

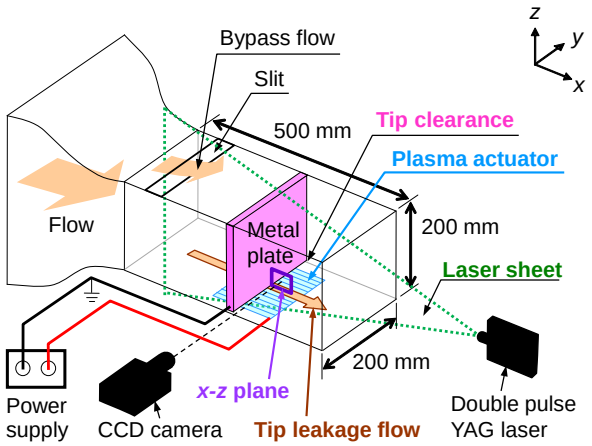

Figure 2. Measurement system for flat plate with tip clearance

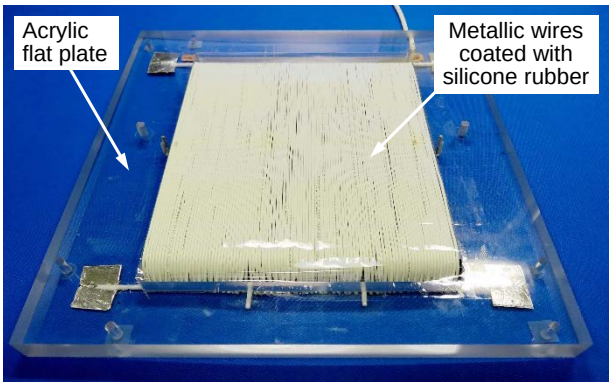

Figure 3. Plasma actuator installed in acrylic flat plate

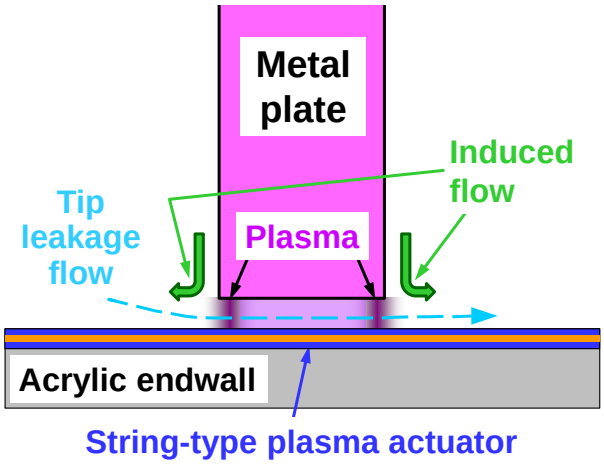

Figure 4. Fundamental mechanism of tip leakage flow reduction by plasma actuator

EXPERIMENTAL RESULTS AND DISCUSSION

Fundamental Mechanism of Tip Leakage Flow Reduction by Plasma Actuator

Figure 4 shows the schematic drawing of the fundamental mechanism of the tip leakage flow reduction by

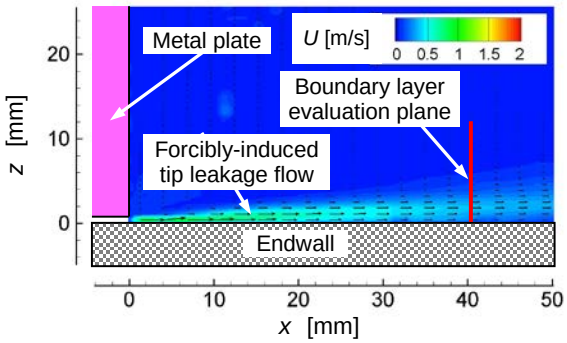

(a) No control

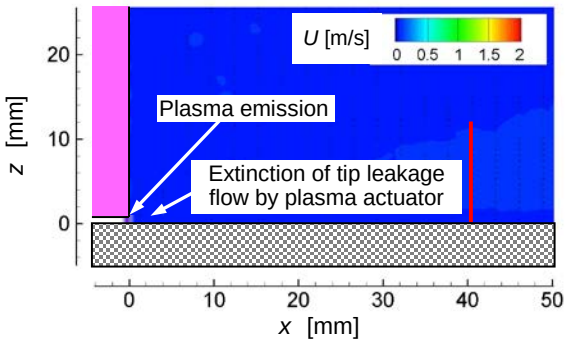

(b) Flow control ($V_{p\text{-}p}$ = 10 kV, f_p = 10 kHz)

Figure 5. Time-averaged absolute velocity distributions near tip clearance exit of flat plate (tip clearance size: 0.6 mm)

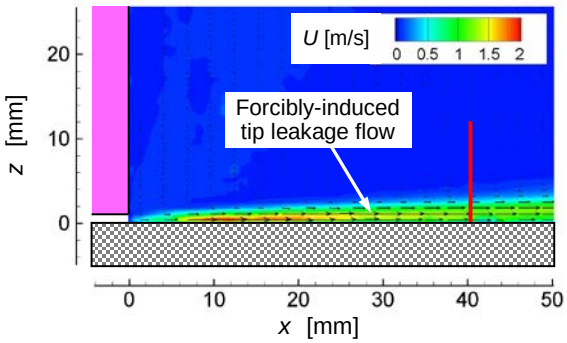

(a) No control

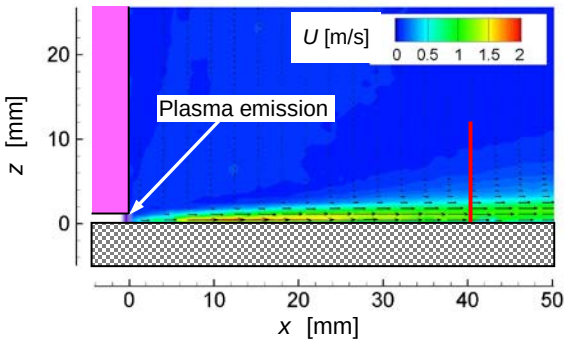

(b) Flow control ($V_{p\text{-}p}$ = 10 kV, f_p = 10 kHz)

Figure 7. Time-averaged absolute velocity distributions near tip clearance exit of flat plate (tip clearance size: 1.0 mm)

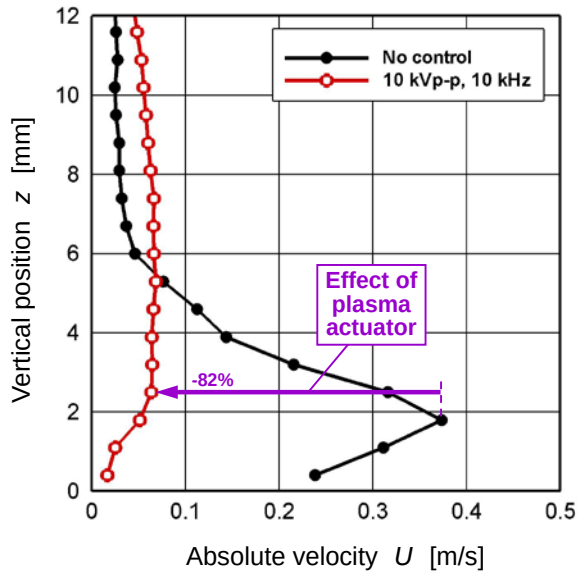

Figure 6. Absolute velocity distributions near tip clearance exit of flat plate at x = 40.5 mm (tip clearance size: 0.6 mm)

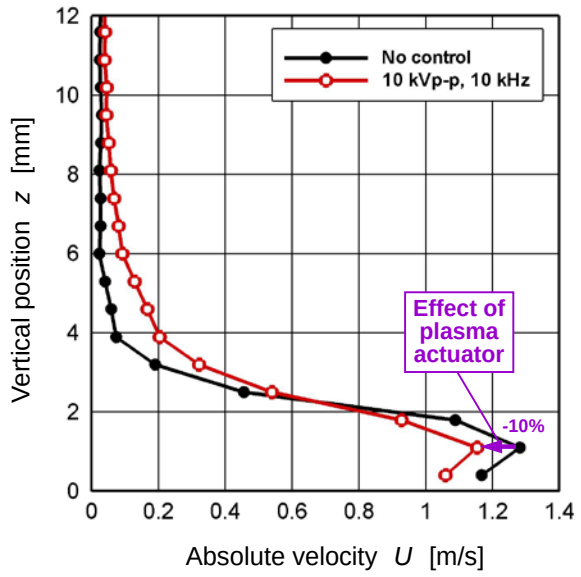

Figure 8. Absolute velocity distributions near tip clearance exit of flat plate at x = 40.5 mm (tip clearance size: 1.0 mm)

the plasma actuator [26]. Due to the plasma actuator operation, the glow discharge plasma is formed between the plasma actuator (metal wires coated with silicone rubber) in the acrylic endwall and the tip of the metal flat plate. The plasma induces the downward flow at each edge of the inlet and outlet of the tip clearance, which blocks the tip leakage flow.

Tip Clearance Size of 0.6 mm

Figure 5 shows the time-averaged absolute velocity distributions near the tip clearance exit of the flat plate of x-z plane (purple frame in Fig. 2) at the tip clearance size of 0.6

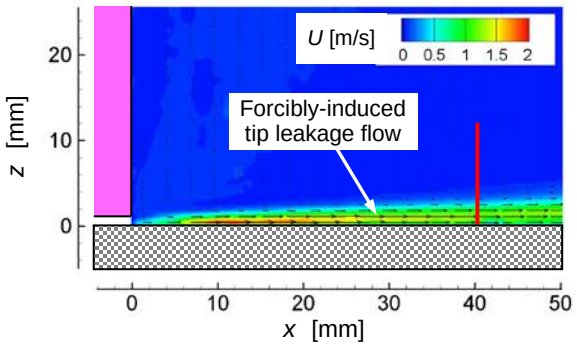

(a) No control

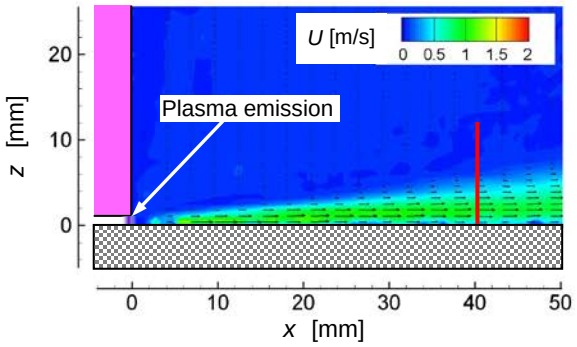

(b) Flow control ($V_{p\text{-}p}$ = 12 kV, f_p = 2 kHz)

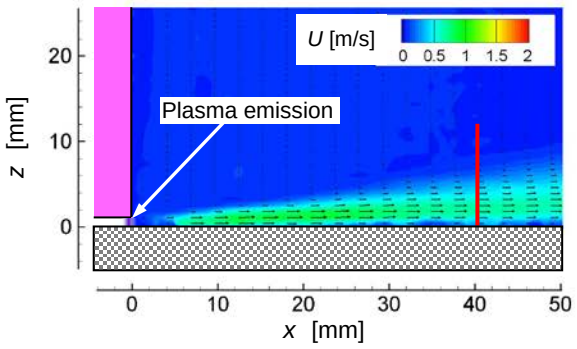

(c) Flow control ($V_{p\text{-}p}$ = 12 kV, f_p = 4 kHz)

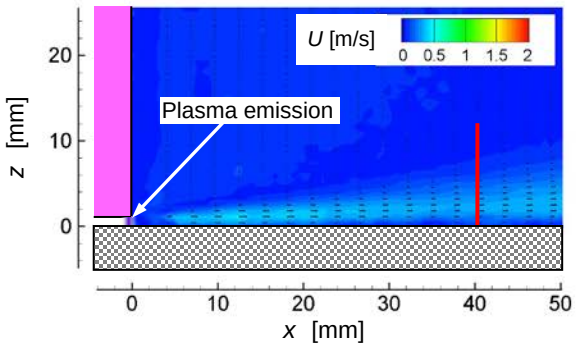

(d) Flow control ($V_{p\text{-}p}$ = 12 kV, f_p = 6 kHz)

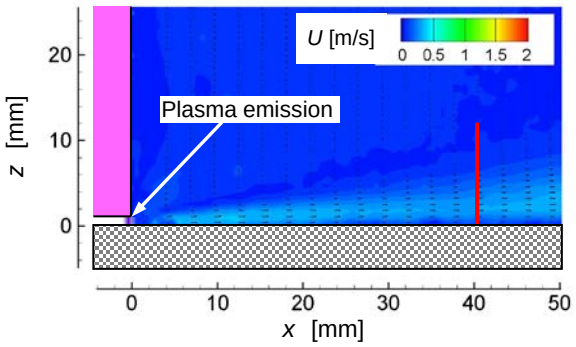

(e) Flow control ($V_{p\text{-}p}$ = 12 kV, f_p = 8 kHz)

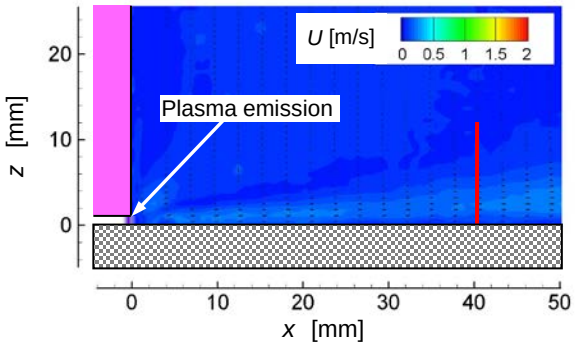

(f) Flow control ($V_{p\text{-}p}$ = 12 kV, f_p = 10 kHz)

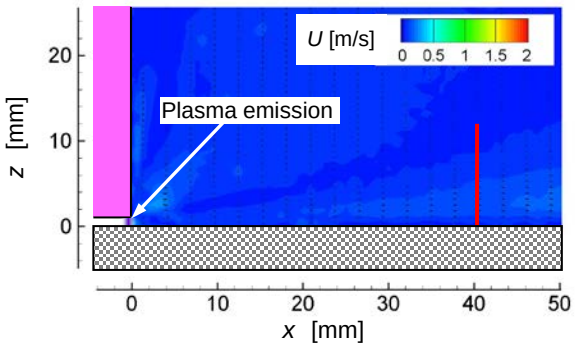

(g) Flow control ($V_{p\text{-}p}$ = 12 kV, f_p = 12 kHz)

Figure 9. Time-averaged absolute velocity distributions near tip clearance exit of flat plate at various DBD-PA input frequencies at constant voltage, $V_{p\text{-}p}$ = 12 kV (tip clearance size: 1.0 mm)

mm. As shown in the no control (baseline) condition in Fig. 5(a), tip leakage flow is forcibly induced through the operation of the wind tunnel. The maximum velocity of the leakage flow at x = 5 mm is approximately 1.0 m/s. As shown in the plasma actuator on condition (input voltage $V_{p\text{-}p}$ = 10 kV, input frequency f_p = 10 kHz) in Fig. 5(b),. the tip leakage flow is dissipated by the plasma actuator operation.

Figure 6 shows the time-averaged absolute velocity distributions near the tip clearance exit of the flat plate at x = 40.5 mm (red lines in Fig. 5). The peak of the absolute velocity of the tip leakage flow is 82% reduced by the effect of the plasma actuator. The flow behind the plate does not go to zero completely because of the mixing and diffusing effects of the induced flow by the plasma actuator (Fig. 4).

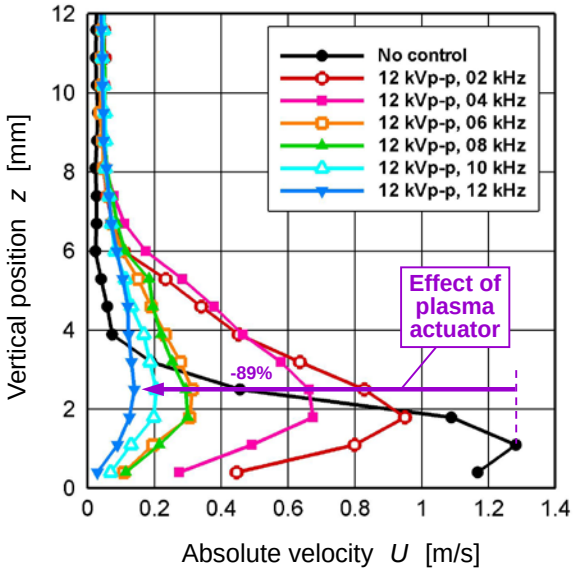

Figure 10. Absolute velocity distributions near tip clearance exit of flat plate at $x = 40.5$ mm at various DBD-PA input frequencies (tip clearance size: 1.0 mm)

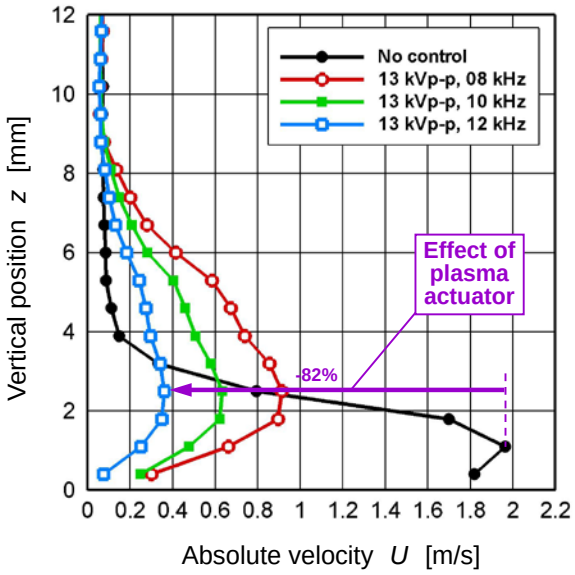

Figure 12. Absolute velocity distributions near tip clearance exit of flat plate at $x = 40.5$ mm at various DBD-PA input frequencies (tip clearance size: 1.4 mm)

Tip Clearance Size of 1.0 mm

Figure 7 shows the time-averaged absolute velocity distributions near the tip clearance exit of the flat plate at the tip clearance size of 1.0 mm. In Fig. 7(a), the maximum velocity of the leakage flow at x = 10 mm is approximately 2.0 m/s. As shown in the plasma actuator on condition, Fig. 7(b),at the same input voltage and frequency condition ($V_{p\text{-}p}$ = 10 kV, f_p = 10 kHz) at the smaller tip clearance size of

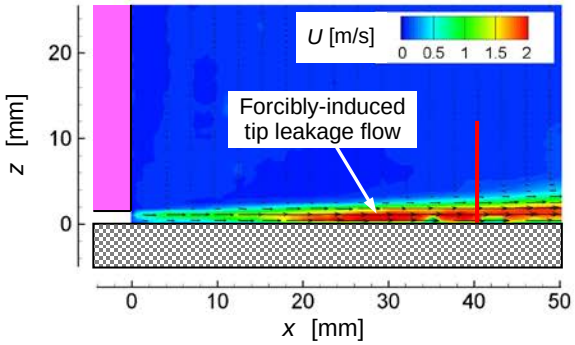

(a) No control

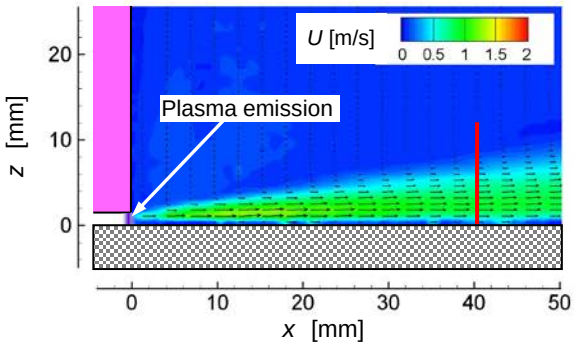

(b) Flow control ($V_{p\text{-}p} = 13$ kV, $f_p = 8$ kHz)

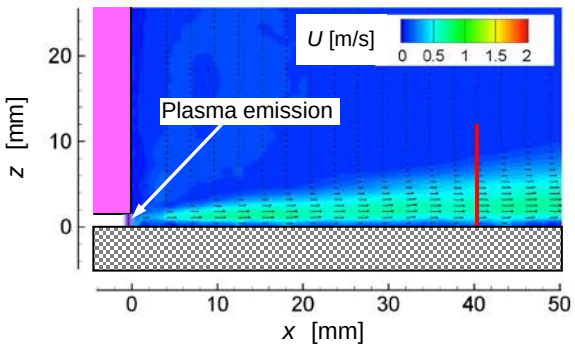

(c) Flow control ($V_{p\text{-}p} = 13$ kV, $f_p = 10$ kHz)

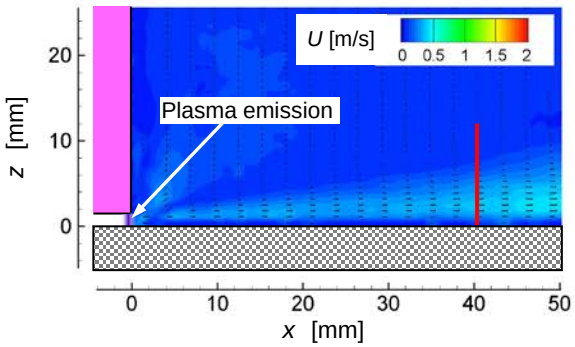

(d) Flow control ($V_{p\text{-}p} = 13$ kV, $f_p = 12$ kHz)

Figure 11. Time-averaged absolute velocity distributions near tip clearance exit of flat plate (tip clearance size: 1.4 mm)

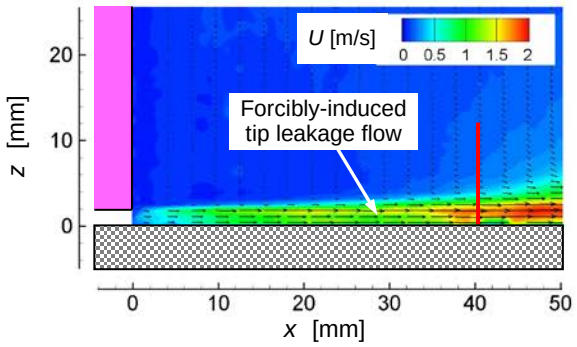

(a) No control

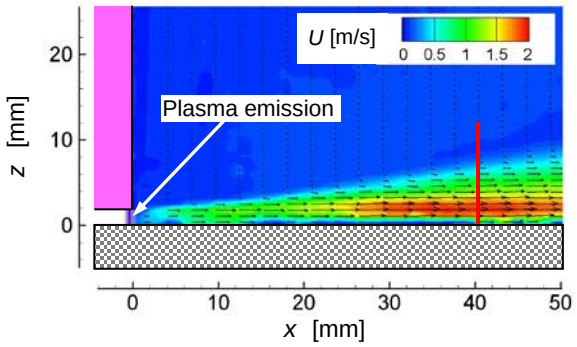

(b) Flow control ($V_{p\text{-}p}$ = 15.5 kV, f_p = 2 kHz)

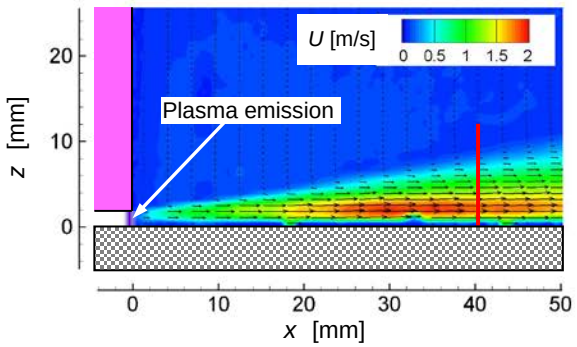

(c) Flow control ($V_{p\text{-}p}$ = 15.5 kV, f_p = 4 kHz)

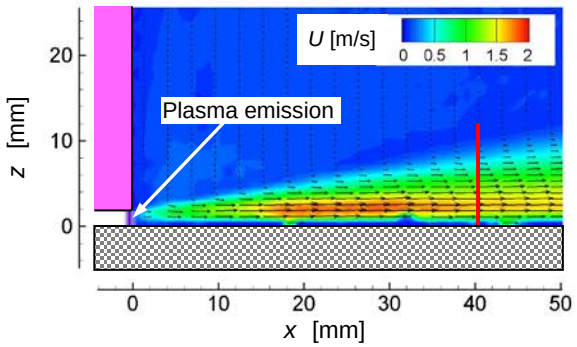

(d) Flow control ($V_{p\text{-}p}$ = 15.5 kV, f_p = 6 kHz)

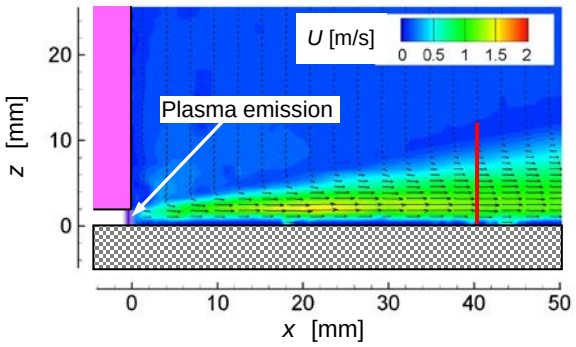

(e) Flow control ($V_{p\text{-}p}$ = 15.5 kV, f_p = 8 kHz)

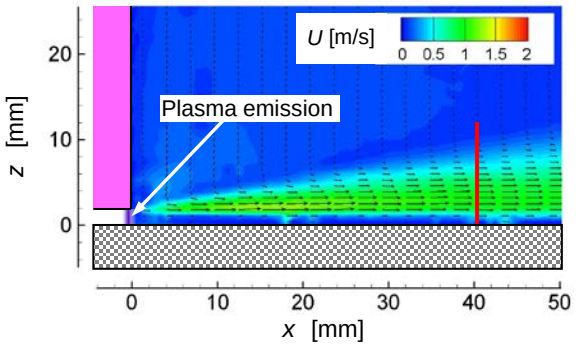

(f) Flow control ($V_{p\text{-}p}$ = 15.5 kV, f_p = 10 kHz)

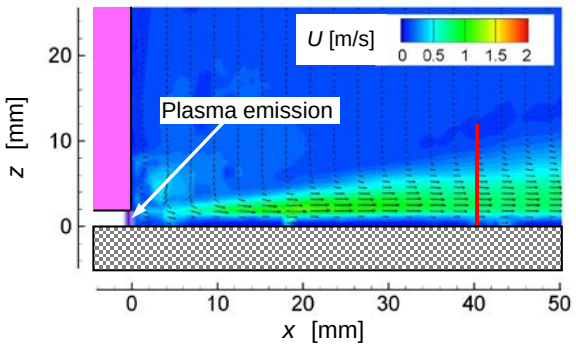

(g) Flow control ($V_{p\text{-}p}$ = 15.5 kV, f_p = 12 kHz)

Figure 13. Time-averaged absolute velocity distributions near tip clearance exit of flat plate at various DBD-PA input frequencies at constant voltage, $V_{p\text{-}p}$ = 15.5 kV (tip clearance size: 1.8 mm)

0.6 mm in Fig. 5(b), the tip leakage flow is slightly reduced by the plasma actuator operation, but the effect of the plasma actuator is considerably smaller than that in Fig. 5(b).

Figure 8 shows the time-averaged absolute velocity distributions near the tip clearance exit of the flat plate at x = 40.5 mm (red lines in Fig. 7). The peak of the absolute velocity of the tip leakage flow is only 10% reduced by the effect of the plasma actuator.

The input voltage and input frequency are changed in order to improve the plasma actuator effects. Figure 9 shows the time-averaged absolute velocity distributions at increased input voltage ($V_{p\text{-}p}$ = 12 kV) at various input frequencies (f_p = 2 kHz - 12 kHz) at the tip clearance size of 1.0 mm. The slight recuction of the peak absolute velocity and the vertical diffusion of the tip leakage flow are observed at the lower input frequencies (Figs. 9(b) and (c)). The tip

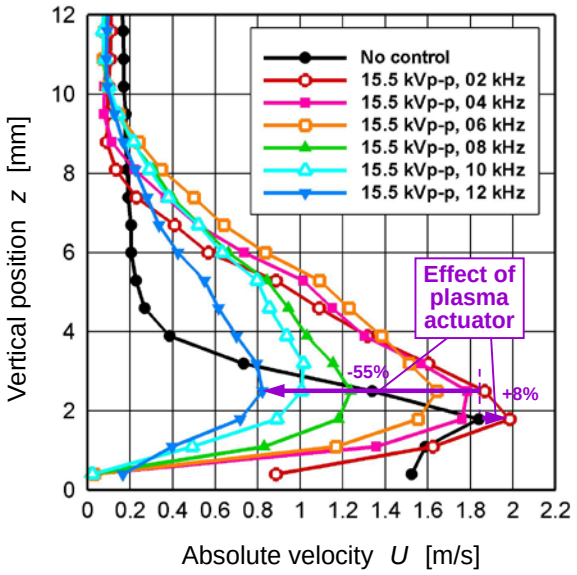

Figure 14. Absolute velocity distributions near tip clearance exit of flat plate at $x = 40.5$ mm at various DBD-PA input frequencies (tip clearance size: 1.8 mm)

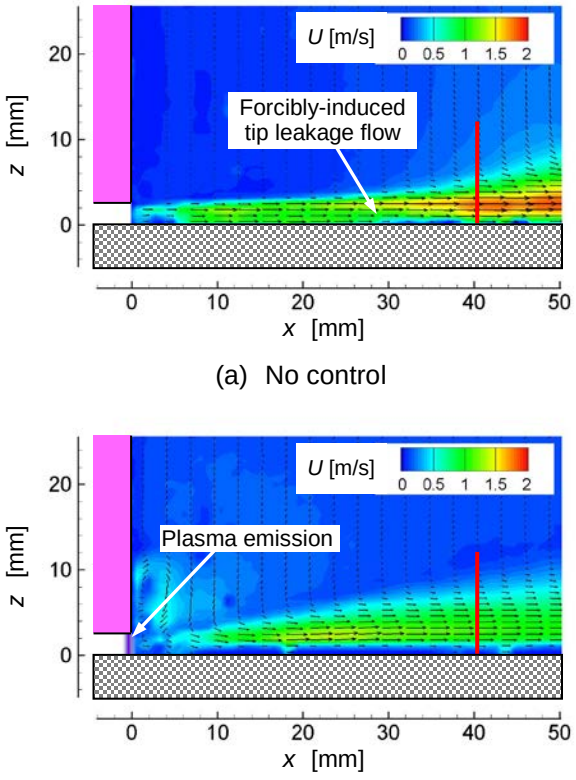

Figure 15. Time-averaged absolute velocity distributions near tip clearance exit of flat plate (tip clearance size: 2.4 mm)

leakage flow is gradually reduced through the active control of the plasma actuator at the higher input frequencies (Figs. 9(d), (e), (f), (g)). At the larger tip clearance size, the higher input voltage is required in order to increase the effect of the plasma actuator.

Figure 10 shows the velocity distributions at x = 40.5 mm at the increased input voltage $V_{p\text{-}p}$ = 12 kV at various input frequencies (red lines in Fig. 9). The peak of the absolute velocity of the tip leakage flow is 89% reduced by the effect of the plasma actuator at the maximum input frequency, f_p = 12 kHz.

Tip Clearance Size of 1.4 mm

Figure 11 shows the time-averaged absolute velocity distributions at increased input voltage ($V_{p\text{-}p}$ = 13 kV) at various input frequencies (f_p = 8 kHz - 12 kHz) at the tip clearance size of 1.4 mm. Due to the increased tip clearance size, the mass flow rate is increased, as shown in Fig. 11(a). The tip leakage flow is gradually reduced at the higher input frequencies, as shown in Figs. 11(b), (c), (d).

Figure 12 shows the velocity distributions at x = 40.5 mm at $V_{p\text{-}p}$ = 13 kV at various input frequencies (red lines in Fig. 11). The tip leakage flow is diffused to the upper direction and is reduced by the plasma actuator operation. The peak velocity of the tip leakage flow is 82% reduced by the effect of the plasma actuator at the maximum input frequency, f_p = 12 kHz.

Tip Clearance Size of 1.8 mm

Figure 13 shows the time-averaged absolute velocity distributions at increased input voltage ($V_{p\text{-}p}$ = 15.5 kV) at various input frequencies (f_p = 2 kHz - 12 kHz) at the larger tip clearance size of 1.8 mm. The slight increase in the

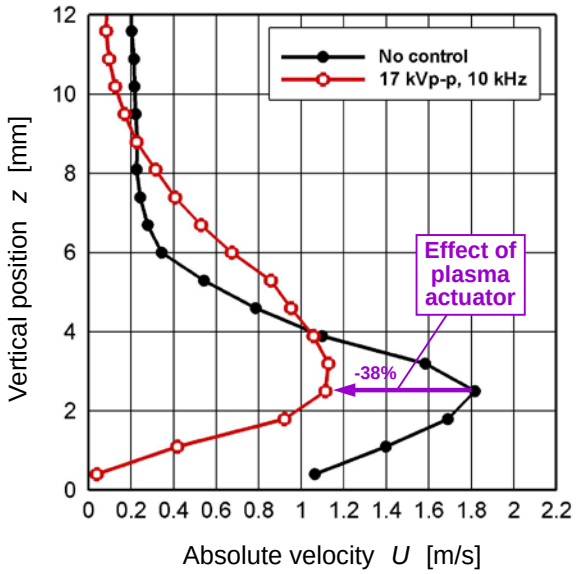

Figure 16. Absolute velocity distributions near tip clearance exit of flat plate at $x = 40.5$ mm (tip clearance size: 2.4 mm)

peak velocity and the large flow diffusion to the upper direction are observed at the lowest input frequencies (f_p = 2 kHz), as shown in Fig. 13(b). The tip leakage flow is

gradually reduced at the higher input frequencies, as shown in Figs. 13(d) - (g).

Figure 14 shows the velocity distributions at x = 40.5 mm at $V_{p\text{-}p}$ = 15.5 kV at various input frequencies (red lines in Fig. 13). At the lowest frequencies (f_p = 2 kHz), the peak veclocity is 8% increased and the tip leakage flow is diffused to the upper direction. At the highest frequencies (f_p = 12 kHz), The peak velocity of the tip leakage flow is 55% reduced by the effect of the plasma actuator.

Tip Clearance Size of 2.4 mm

Figure 15 shows the time-averaged absolute velocity distributions at increased input voltage ($V_{p\text{-}p}$ = 17 kV) at the largest tip clearance size of 2.4 mm. The reduction of the peak velocity and the flow diffusion to the upper direction are observed at the plasma actuator operation (f_p = 10 kHz), as shown in Fig. 15(b).

Figure 16 shows the velocity distributions at x = 40.5 mm (red lines in Fig. 15) at $V_{p\text{-}p}$ = 17 kV at the tip clearance size of 2.4 mm. The peak velocity of the tip leakage flow at $V_{p\text{-}p}$ = 17 kV and f_p = 10 kHz is only 38% reduced by the effect of the plasma actuator.

CONCLUSIONS

Ring-type dielectric barrier discharge (DBD) plasma actuators have been developed for active control of the tip leakage flow in a turbine rotor. Here, the ring-type plasma actuators consisted of metallic wires coated with insulation material, mounted in an insulator embedded in the tip casing wall. For the fundamental experiments involving a flat plate with tip clearance, the two-dimensional velocity fields near the plate and blade tip regions were measured using particle image velocimetry (PIV). In this study, effects of the tip clearance size of the flat plate were examined at different tip clearance sizes from 0.6 mm to 2.4 mm in a wind tunnel at low tip leakage velocity conditions of 1 m/s - 2 m/s.. The input voltage and frequency were varied in the ranges between 10 kV and 17 kV, 2 kHz and 12 kHz, respectively.

The forcibly-induced tip leakage flow was easily dissipated at smaller tip clearance size (0.6 mm and 1.0 mm) by applying relatively smaller input voltage. The larger tip clearance size requires the higher applied voltage and frequency in order to reduce the tip leakage flow. At larger tip clearance of 1.8 mm, the mass flow rate of the tip leakage flow is increased and the flow diffusion is observed at the low frequency operation, 2 kHz. At the largest tip clearance of 2.4 mm, the peak velocity of the tip leakage flow is 38% reduced by the effect of the plasma actuator of the input voltage of 17 kV and frequency of 10 kHz.

The flow velocity and pressure gradient of actual turbines are much higher than those of the low-speed flat plate experiments in this research. In general, the tip leakage flow reduction in the higher-speed condition demands more electric power. Higher-speed experiments and optimizations of the plasma actuator operation methods are required.

ACKNOWLEDGMENTS

This work was supported by JSPS KAKENHI, Grant-in-Aid for Scientific Research (B), Grant Number 26289040.

REFERENCES

[1] Booth,, T. C., “Importance of Tip Clearance Flows in Turbine Design,” von Karman Institute for Fluid Dynamics, Lecture Series 1985-05, Tip Clearance Effects in Axial Turbomachines, pp. 1-34, 1985.

[2] Sjolander, S. A., “Overview of Tip-Clearance Effects in Axial Turbines,” von Karman Institute for Fluid Dynamics, Lecture Series 1997-01, Secondary and Tip-Clearance Flows in Axial Turbines, pp. 1-29, 1997.

[3] Bindon, J. P., “The Measurement and Formation of Tip Clearance Loss,” Transactions of ASME Journal of Turbomachinery, 111, pp. 257-263, 1989.

[4] Dishart, P. T., and Moore, J., “Tip Leakage Losses in a Linear Turbine Cascade,” Transactions of ASME Journal of Turbomachinery, Vol. 112, pp. 599-608, 1990.

[5] Yaras, M., and Sjolander, S. A., “Development of the Tip-Leakage Flow Downstream of a Planar Cascade of Turbine Blades: Vorticity Field,” Transactions of ASME Journal of Turbomachinery, Vol. 112, pp. 609-617, 1990.

[6] Heyes, F. J. G., and Hodson, H. P., “Measurement and Prediction of Tip Clearance Flow in Linear Turbine Cascade,” Transactions of ASME Journal of Turbomachinery, Vol. 115, pp. 376-382, 1993.

[7] Heyes, F. J. G., Hodson, H. P., and Dailey, G. M., “The Effect of Blade Tip Geometry on the Tip Leakage Flow in Axial Turbine Cascades,” Transactions of ASME Journal of Turbomachinery, Vol. 114, pp. 643-651, 1992.

[8] Morphis, G., and Bindon, J. P., “The Performance of a Low Speed One and Half Stage Axial Turbine with Varying Rotor Tip Clearance and Tip Gap Geometry,” ASME Paper No. 94-GT-481, 1994.

[9] Ainley, D. G., and Mathieson, G. C. R., “A Method of Performance Estimation for Axial-Flow Turbines,” A.R.C. Technical Report R&M, No. 2974, 1951.

[10] Dunham, J., and Came, P. M., “Improvements to the Ainley-Mathieson Method of Turbine Performance Prediction,” Transactions of ASME Journal of Engineering for Power, Vol. 92, pp. 252-256, 1970.

[11] Lakshminarayana, B., 1970, “Methods of Predicting the Tip Clearance Effects in Axial Flow Turbomachinery,” Transactions of ASME Journal of Basic Engineering, pp. 467-482, 1970.

[12] Kacker, S. C., and Okapuu, U., “A Mean Line Prediction Method for Axial Flow Turbine Efficiency,” Transactions of ASME Journal of Engineering for Power, Vol. 104, pp. 111-119, 1982.

[13] Yaras, M. I., and Sjolander, S. A., “Prediction of Tip-Leakage Losses in Axial Turbines,” Transactions of ASME Journal of Turbomachinery, Vol. 114, pp. 204-210, 1992.

[14] Denton, J. D., “Loss Mechanisms in Turbomachines,”

Transactions of ASME Journal of Turbomachinery, Vol. 115, pp. 621-656, 1993.

[15] Roth, J. R., Sherman, D. M., and Wilkinson, S. P., "Boundary Layer Flow Control with a One Atmosphere Uniform Grow Discharge," AIAA Paper, No. 98-0328, 1998.

[16] Corke, T. C., Enloe, C. L., and Wilkinson, S. P., "Dielectric Barrier Discharge Plasma Actuators for Flow Control," Annual Review of Fluid Mechanics, Vol. 42, pp. 505-529, 2010.

[17] Post M. L., Corke, T. C., "Separation Control on High Angle of Attack Airfoil Using Plasma Actuators," 45th AIAA Aerospace Sciences Meeting and Exhibit, Reno, NV, 6-9 January 2003, AIAA 2003-1024.

[18] Labergue, A., Moreau, E., Zouzou, N., Touchard, G., "Separation Control Using Plasma Actuators: Application to a Free Turbulent Jet," Journal Physics D: Applied Physics, Vol. 40, 2007, pp. 674-684.

[19] Asada, K., Ninomiya, Y., Oyama, A., Fujii, K., "Airfoil Flow Experiment on The Duty Cycle of DBD Plasma Actuator," 47th AIAA Aerospace Sciences Meeting, Orlando, FL, 5-8 January 2009, AIAA 2009-531.

[20] Segawa, T., Yoshida, H., Takekawa, S., Jukes, T., Choi, K-S., "Generation of Functional Jet Using DBD Plasma Actuator with Facing Linear Electrodes," Theoretical and Applied Mechanics, Vol. 57, 2009, pp.289-296.

[21] Walker, R. S., Segawa, T., "Mitigation of Flow Separation Using DBD Plasma Actuators on Airfoils: A Tool for More Efficient Wind Turbine Operation," Renewable Energy, Vol. 42, 2012, pp. 105-110.

[22] Choi, K-S., Jukes, T., and Whalley, R., "Turbulent Boundary-Layer Control with Plasma Actuators," Philosophical Transactions of the Royal Society A, Vol. 369, 2011, pp. 1443-1458.

[23] Van Ness II, D. K., Corke, T. C., and Morris, S. C., "Turbine Tip Clearance Flow Control using Plasma Actuator," AIAA Paper, No. 2006-0021, 2006.

[24] Van Ness II, D. K., Corke, T. C., and Morris, S. C., "Stereo PIV of a Turbine Tip Clearance Flow with Plasma Actuation," AIAA Paper, No. 2007-647, 2007.

[25] Van Ness II, D. K., Corke, T. C., and Morris, S. C., "Tip Clearance Flow Visualization of a Turbine Blade Cascade with Active and Passive Control," ASME Paper, No. GT2008-50703, 2008.

[26] Matsunuma, T., and Segawa, T., "Active Tip Clearance Control for an Axial-flow Turbine Rotor Using Ring-Type Plasma Actuators," ASME Paper, No. GT2014-26390, 2014.